Chromatofocusing of Peptides and Proteins Using Linear pH Gradients Formed on Strong Ion-Exchange Adsorbents

Xuezhen Kang,* Douglas D. Frey

Department of Chemical and Biochemical Engineering, University of Maryland Baltimore County, Baltimore, Maryland 21250; telephone: (410) 455-3418 fax: (410) 455-6500; e-mail: dfrey1@umbc.edu

Received 30 April 2003; accepted 28 August 2003

Published online 9 July 2004 in Wiley InterScience (www.interscience.wiley.com). DOI: 10.1002/bit.20122

Abstract: Although it is commonly believed that a column packing used for chromatofocusing must have an "even" buffering capacity in order to produce a linear pH gradient, it is demonstrated here that linear pH gradients suitable for chromatofocusing can be produced on a column packing having a minimal buffering capacity. In particular, if either a strong-acid cation-exchange column packing or a strong-base anion-exchange column packing is presaturated with either a weak acid titrated with a strong base, or a weak base titrated with a strong acid, respectively, to the initial pH, then a linear or nearly linear pH gradient can be formed using a polyampholyte elution buffer by taking advantage of the presence of small quantities of weak-acid or weak-base functional groups that generally exist on these types of column packings. Experimental and theoretical studies are used to demonstrate that such systems have potential advantages over traditional chromatofocusing methods in terms of the speed of the separation, the resolution achieved, and the range of applications possible. Among other techniques described, a method for separating tryptic peptides using chromatofocusing and a strong-acid cation-exchange column packing is demonstrated to be a useful alternative to capillary isoelectric focusing and ion-exchange chromatography using a salt gradient for this purpose. © 2004 Wiley Periodicals, Inc.

Keywords: chromatofocusing; peptides; proteins; ion exchange

INTRODUCTION

Chromatofocusing is an ion-exchange chromatography (IEC) method which employs an internally produced, retained pH gradient that travels through the column more slowly than an unadsorbed eluite. One of the most widely held beliefs related to the technique is that in order to achieve a linear pH gradient, the elution buffer and column packing must both "give an even buffering capacity across a broad pH range" (Amersham Pharmacia Biotech, 1981). The wide acceptance of this generalization is surprising given the fact that Sluyterman and Elgersma (1978) in their original work describing chromatofocusing concluded that the ratio of the buffering capacities in the mobile and stationary phases should vary linearly with pH to form a linear gradient. A more rigorous derivation of the case considered by Sluyterman and Elgersma where the propagation of the gradient results from the transfer of a strong base from the mobile phase to the stationary phase was given by Bates et al. (2000), who came to the same conclusion provided that the change in pH in the mobile and stationary phases is congruent, i.e., $dpH_{fluid}/dpH_{ads} = 1$. It was subsequently shown by Kang (2002) that congruency is approximately valid for most ion-exchange column packings. Kang and Frey (2002) also conducted experiments using a weak-base anion-exchange column packing and a simple mixture of weak-base buffering species that form only cationic species and confirmed that a linear pH gradient is formed when the ratio of the buffering capacities in mobile and stationary phases varies linearly with pH.

Although chromatofocusing employing a polyampholyte buffer does not strictly conform to the above restriction that only inert ions are adsorbed, where an inert ion is defined to be an ion not participating in acid–base equilibrium, it was nevertheless shown theoretically by Frey et al. (1995, 2002) that linear or nearly linear pH gradients can be produced using a strong-base anion-exchange column packing having no buffering capacity, provided that the packing is first presaturated with an adsorbed buffering species (i.e., with a weak acid for the case of an anion-exchange column packing), and then eluted with a polyampholyte buffer. This further indicates that an "eveness" for the column packing buffering capacity is not required to produce a linear pH gradient in chromatofocusing. In the present study, a related system is investigated in which linear pH gradients are formed on either a strong-base or strong-acid ion-exchange column packing having a minimal buffering capacity by first presaturating the column with an inert adsorbed ion, and by then taking advantage of the presence of small amounts of weak-acid or weak-base functional groups on the packing. Such systems are shown to have a number of useful potential advantages as compared to standard chromatofocusing methods.

Correspondence to: D.D. Frey
*Current address for X. Kang: Genzyme Corp., Framingham, MA 01701
Contract grant sponsor: National Science Foundation
Contract grant number: CTS 9813658

MATERIALS AND METHODS

Citric acid, NaH_2PO_4, MOPS (3-[N-morpholino]propanesulfonic acid), acetic acid, diethanolamine, Trizma base (Tris, tris[hydroxymethyl]aminomethane), NaCl, and Polybuffers 96 and 74 were obtained from Sigma (St. Louis, MO). HPLC-grade acetonitrile was obtained from Fisher (Pittsburgh, PA). To make the buffers, mixtures of the buffer components were titrated with NaOH or HCl to the desired pH and the mixture was then vacuum filtered. The columns used were a 5 × 0.5 cm I.D. Mono P weak-base anion-exchange column and a Mono Q strong-base anion-exchange column of the same size, both obtained from Amersham Biosciences (Piscataway, NJ), a 7.5 × 0.75 cm I.D. TSK-GEL Q-5PW strong-base anion-exchange column obtained from Toso Bioscience (Montgomeryville, PA), and a 10 × 0.46 cm I.D. PolySULFOETHYL A strong-acid cation-exchange column obtained from PolyLC (Columbia, MD). According to the manufacturer, this last column contains 5 μm particles with 300 Å pores and is covalently coated with poly(2-sulfoethylaspartamide), which produces a highly hydrophilic surface appropriate for mixed-mode electrostatic-hydrophilic interaction chromatography.

Ovalbumin, bovine serum albumin (BSA), β-lactoglobulin A (Lac A), bovine hemoglobin, bovine cytochrome C, the peptides listed in Table III (described later), human hemoglobins A_0 and S_1, and TPCK-treated trypsin were all obtained from Sigma. To digest a protein using trypsin, the protein was first dissolved in 100 mM Tris-HCl at pH 8.5 and a ratio of 1:50 (w/w) of enzyme to substrate was used. The trypsin solution, which was prepared by dissolving the trypsin in 1 mM HCl to a concentration of 1 mg/mL, was added to the substrate protein solution and the resulting mixture was incubated at 37 °C for 24 h. No effort was made to remove the heme group from cytochrome C or hemoglobin prior to the digestion. The protein digest, diluted using the presaturation buffer to a certain concentration, was used as the sample.

The chromatography equipment used was a Model P4000 SpectraSystem pump and a Model UV2000 SpectraSystem UV-Vis absorbance detector (Thermo Separation Products, San Jose, CA). The chromatography system was equipped with a low-dead-volume, in-line pH sensing cell (Sensorex, Stanton, CA) and a Model 701A Ionanalyzer (Orion, Beverly, MA) to record the pH of the column effluent. Sample introduction and the formation of a stepwise change from the presaturation buffer to the elution buffer at the column inlet was accomplished using two Model 9010 valves (Rheodyne, Rohnert Park, CA).

RESULTS AND DISCUSSION

Formation of pH Gradients on a Strong-Base Ion Exchange Column Packing Using Polyampholytes

Figure 1 illustrates calculations adapted from Frey et al. (2002) performed using the numerical method of characteristics and using conditions representative of those commonly used for chromatofocusing on a weak-base anion-exchange column packing, except that the polyampholyte elution buffer is replaced by a mixture of five weak-acid buffering species (species A_1 to A_5) and one weak-base buffering species (species B_1). The figure specifically shows the effluent values for the pH and the total concentration of each buffering species (i.e., the sum of the concentrations of all forms of each buffering species) as a function of the dimensionless time. Details of the calculation procedure are given in the Appendix.

In the calculation shown in Figure 1 the column is presaturated with a weak base titrated to the initial pH using a strong acid that produces the conjugate base I^-, where I^- denotes an inert ion that does not participate in acid–base equilibrium, such as the chloride ion. As illustrated, each adsorbed buffering species in the elution buffer, i.e., each weak acid, leads to the formation of one self-sharpening pH front. Correspondingly, for the case of a polyampholyte buffer containing many adsorbed buffering species, a very large number of small stepwise pH fronts would be formed so that a linear pH gradient is produced. The numerical calculation shown also illustrates several commonly observed features that result when standard conditions for chromatofocusing are employed, such as a decrease in the pH in the middle of the gradient to a level below that of the elution buffer.

The results shown in Figure 1 where a weak-base anion-exchange column packing is employed can be compared to those shown in Figure 2, which illustrates numerical calculations for the case of a strong-base anion-exchange column packing where the column is first presaturated with a weak-base buffering species titrated to the presaturation pH by a strong acid which produces the conjugate base I^-, and then eluted with a mixture containing two weak-acid buffering species titrated to the final pH using a strong base which produces the conjugate acid I^+. As shown, an initial pH increase is observed due to the interactions of I^-, I^+, and the weak base B_1. This initial pH change is largely absent in Figure 1 due to the different elution and presaturation buffers used, and because of the presence in that figure of relatively large amounts of weak-base functional groups on the column packing. It can also be seen in Figure 2 that, even though the weak-base buffering species B_1 does not form an anionic species upon dissociation, it is retained to some extent by the column packing due to the adsorption of the neutral form of this species. After the initial pH rise, the pH in Figure 2 decreases to a value much lower than the elution pH in a stepwise change which results from the rapid decrease in the concentration of species B_1 and a corresponding rapid increase in the concentrations of species A_1 and A_2. Finally, the pH increases slowly to the elution pH due to the decrease in the concentration of the species I^-.

Although the pH gradient shown in the top part of Figure 2 is not useful for chromatofocusing due to the steepness of the decreasing section, this section can be seen nevertheless to be composed of two distinct stepwise

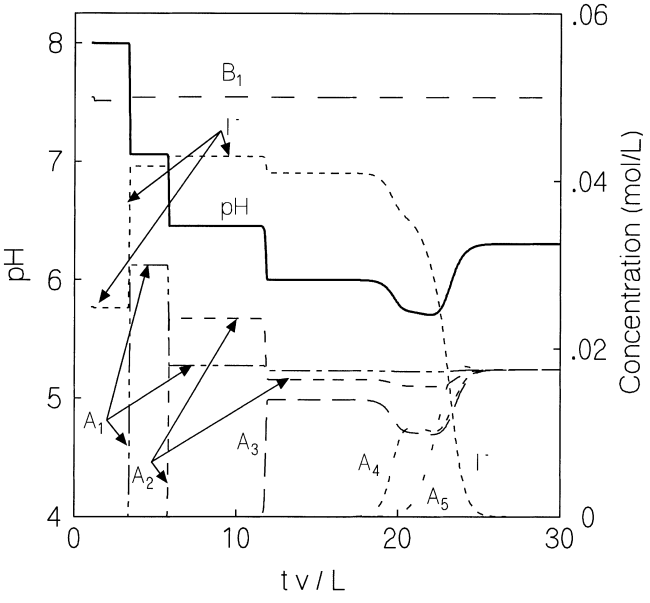

Figure 1. Effluent pH and buffering species concentration profiles for a weak-base anion-exchange column packing where $\alpha = 0.35$, $\epsilon = 0$, $v_{fluid} = 0.06$ cm/s, $L = 10$ cm, $d_p = 45$ μm. It was assumed there were 15 types of functional groups on the column packing, with 14 of the groups each having concentrations of 0.026 M and pK_a values evenly spanning the range from 3 to 9.5 and with the final functional group being strongly basic and having a concentration of 0.43 M. I^- denotes an inert anion, A_1 to A_5 denote weak-acid buffering species with pK_a values of 8, 7, 6, 5, and 4, respectively, and B_1 denotes a weak-base buffering species with a pK_a value of 8.0. The column was presaturated at pH 8 with 0.05 M B_1 and 0.025 M I^- and eluted with 0.05 M B_1 and 0.0175 M of all the acidic buffering species at pH 6.5. $K_{A_i^-,ads} = K_{A_i^o,ads} = K_{A_i^+,ads} = 1$ for all species, and $D_{eff} = 8 \times 10^{-7}$ cm^2/s for all buffering species. The curves shown for each buffering species denote the sum of all the charged forms of that buffering species.

changes, as illustrated in the bottom part of Figure 2, where the time scale is expanded. It is therefore of interest to investigate the effect of small amounts of weak-base functional groups attached to an otherwise strong-base column packing since such groups are generally present, and their titration behavior will influence the shape of the steep pH section shown. To explore this effect, Figure 3 shows the calculated pH and buffering species concentration profiles in the column effluent with the same conditions as in Figure 2, but assuming that the column packing consists of 90% strong-base functional groups and 10% weak-base functional groups having a pK_a of 6.5. As shown in the figure, although the pH of the column effluent also initially decreases to a value lower than pH of the elution buffer, this value is much higher than in Figure 2. The bottom part of Figure 3 illustrates the pH and composition profiles for the initial part of the gradient using an expanded time scale. It can be seen in the figure that a pH plateau occurs between the two stepwise pH changes, and buffering species A_1 adsorbed onto the column packing is displaced from the column by buffering species A_2, similar to the way buffering species are displaced in sequence in Figure 1. This suggests that the conditions used in Figure 3 constitute a new strategy for producing stepwise pH changes on a strong-base anion exchanger when using simple buffers, and therefore also a new strategy for performing chromatofocusing with linear pH gradients when using a polyampholyte buffer.

To evaluate experimentally the hypothesis that the conditions illustrated in Figure 3 are useful in practice, the strong-base anion-exchange column packing TSK-Gel Q-5PW was presaturated and eluted using conditions similar to those in Figure 2, with the resulting pH gradient shown in Figure 4. As illustrated, a rapid, stepwise change in pH down to pH 4 was observed, after which the pH increases slowly to the elution pH of 4.5 over a prolonged time period, similar to the results shown in Figure 3. The bottom part of Figure 4 shows the initial part of the pH gradient using an expanded time scale. As illustrated, the steep downward pH change observed in the top part of Figure 4 is actually composed of two stepwise changes separated with a pH plateau. Furthermore, when the time scale is presented in terms of the dimensionless group tv/L, the experimental results in Figure 4 are in good agreement with the calculated results in Figure 3.

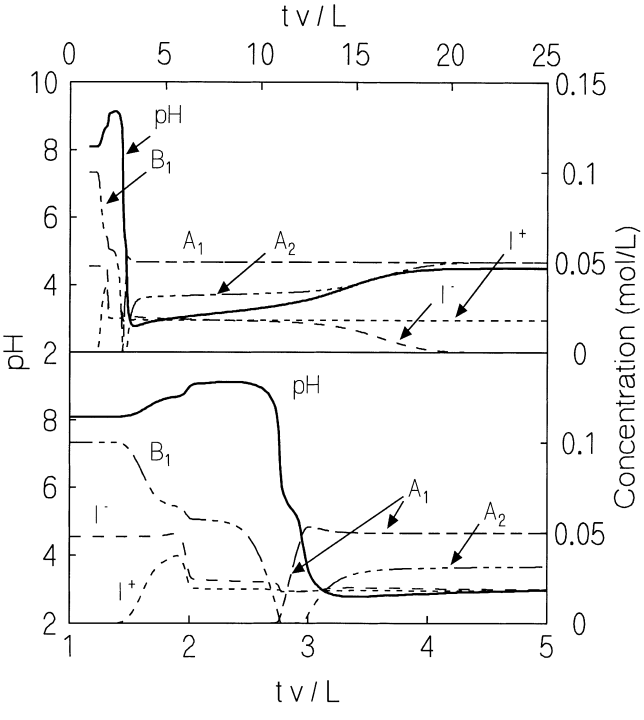

Figure 2. Effluent pH and buffering species concentration profiles for a strong-base anion-exchange column packing where $\alpha = 0.35$, $\epsilon = 0$, $v_{fluid} = 0.054$ cm/s, $L = 7.5$ cm, $d_p = 45$ μm. It was assumed there was one type of strongly basic functional group on the column packing with a concentration of 0.15 M. I^+ and I^- denote an inert cation and an inert anion, respectively. A_1 and A_2 denote weak-acid buffering species with pK_a values of 7.2 and 4.75, respectively, and B_1 denotes a weak-base buffering species with pK_a value of 8.06. The column was presaturated at pH 8.1 with 0.1 M B_1 and 0.048 M I^- and eluted at pH 4.5 with 0.018 M I^+ and 0.05 M each of A_1 and A_2. $K_{A_i^-,ads} = K_{A_i^o,ads} = K_{A_i^+,ads} = 1$ for all species, $D_{eff} = 7.6 \times 10^{-7}$ cm^2/s for A_1 and B_1, and $D_{eff} = 8.3 \times 10^{-7}$ cm^2/s for A_2. The curves shown for each buffering species denote the sum of all the forms of that buffering species. Top: the whole gradient. Bottom: the initial part of the gradient.

The results in this section suggest that the presence of small quantities of weak-electrolyte groups on an otherwise strong-electrolyte column packing can be used as the basis for forming a gradual pH gradient suitable for chromatofocusing. Although the exact shape of the pH gradient formed in this way will depend to some extent on the properties of the weak-electrolyte functional groups present, in the following sections it will be demonstrated that in many cases the gradient shape is sufficiently linear to produce useful separations. Furthermore, the results in this section suggest that such systems may have advantages over traditional chromatofocusing systems, since both the gradient velocity and column packing charge density will be higher for a given pH and polyampholyte concentration, which should result in higher separation speeds and resolution.

Separation of Proteins

The top part of Figure 5 shows the pH gradient produced using the method described above with a Mono Q strong-base anion-exchange column and with Polybuffer 96 as the eluent. As shown, after an initial small decrease in pH, a nearly linear pH gradient is obtained. The linear section of the pH gradient can be explained as discussed in the previous section by the fact that Polybuffer 96 is composed of a large number of buffering species with evenly distributed pK_a values in the pH range of approximately 6 to 9, so that a large number of small stepwise pH fronts are formed in this range, and therefore a linear pH gradient is observed. The initial pH decrease is evidently caused by the replacement of the diethanolamine in the presaturation buffer with the positively charged components of the Polybuffer at pH 9. Also shown in the figure is the separation of a mixture of human hemoglobins A_0 and S_1. As illustrated, the two variants are completely separated, and four minor peaks are also observed.

In order to compare the resolution achieved using the Mono Q strong-base column packing to that achieved using a weak-base column packing as traditionally employed in chromatofocusing, the same buffer system was used to separate the same proteins as in the top part of Figure 5, but by using instead a weak-base column packing specifically intended for chromatofocusing (i.e., the Mono P column) at two different flow rates. As shown in the middle and bottom parts of Figure 5, a pH gradient was produced using the Mono P column that is similar in shape to that produced using the Mono Q column.

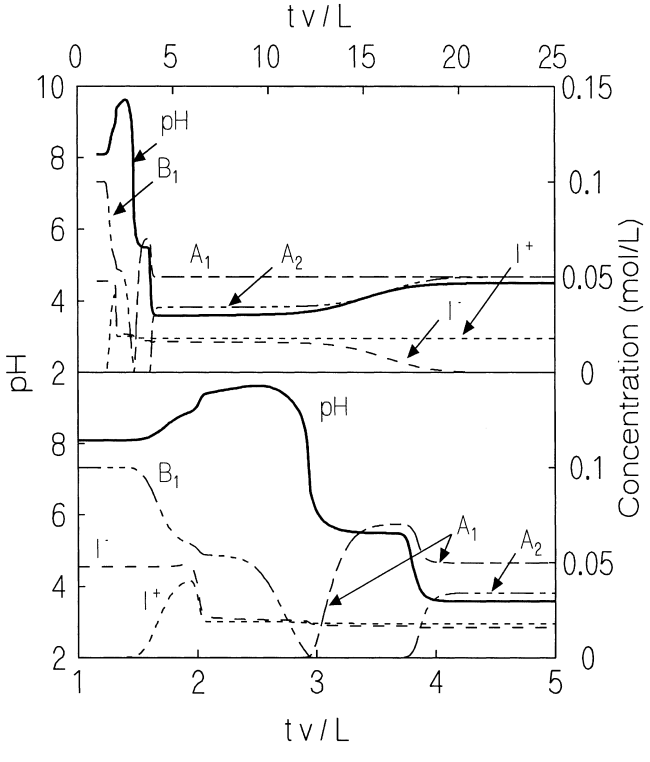

Figure 3. Effluent pH and buffering species concentration profiles for an anion-exchange column packing where $\alpha = 0.35$, $\epsilon = 0$, $v_{fluid} = 0.06$ cm/s, $L = 10$ cm, $d_p = 45$ μm. It was assumed the column packing was functionalized with 0.15 M ion-exchange functional groups, 90% of which are strongly basic and 10% are weakly basic having a pK_a of 6.5. Other conditions are the same as in Figure 2. The curves shown for each buffering species denote the sum of all the forms of that buffering species. Top: the whole gradient. Bottom: the initial part of the gradient.

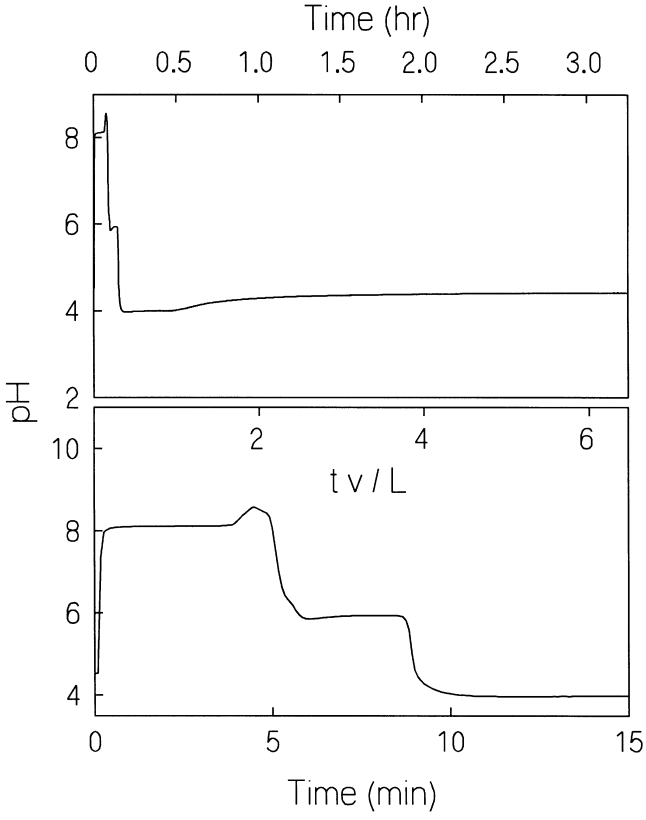

Figure 4. pH gradient formed on a Q-5PW strong-base anion-exchange column. The column was presaturated with 100 mM Tris titrated to pH 8.1. The elution buffer was composed of 50 mM each of MOPS and acetic acid at pH 4.5. The flow rate was 0.5 mL/min. Top: the whole gradient. Bottom: the initial part of the gradient.

Since the mass of protein in the sample was the same for all three cases shown in Figure 5, the higher peak height obtained with the Mono Q column indicates that the proteins are more highly concentrated and occupy a smaller volume in that column as compared to the Mono P column. The more focused bands achieved using the Mono Q column is likely due to the higher charge density on this packing, and therefore the higher Donnan potential obtained, since according to Sluyterman and Elgersma (1978) the band width decreases with the Donnan potential. Furthermore, when using the Mono P column packing, a reduction in pH causes an increase in the charge density of the column packing, which partially reduces the effectiveness of the pH gradient to elute proteins and produce a focusing effect. In contrast, for the strong-base Mono Q column packing, the charge density remains constant so that the pH gradient is more effective for elution.

Despite the smaller volume occupied by the proteins bands when using the Mono Q column, it can be seen by comparing the top and bottom parts of Figure 5 that the resolutions achieved using the Mono Q and Mono P columns at the same flow rate are not significantly different, since the more highly focused and more symmetrical bands obtained using the Mono Q column is compensated for to a large degree by a greater spacing between bands, i.e., a greater adsorption selectivity, obtained with the Mono P column. However, the figure also indicates that at the same flow rate the separation time is shorter when using the Mono Q column due to the higher velocity of the pH gradient. For comparison purposes, the middle part of Figure 5 shows the separation obtained using the Mono P column at a flow rate that yields nearly the same separation time achieved using the Mono Q column. As indicated by comparing the top and middle parts of Figure 5, the Mono Q column achieves a higher resolution than the Mono P column when the separation times are comparable, which is the most common basis for comparing the resolving ability of two different columns.

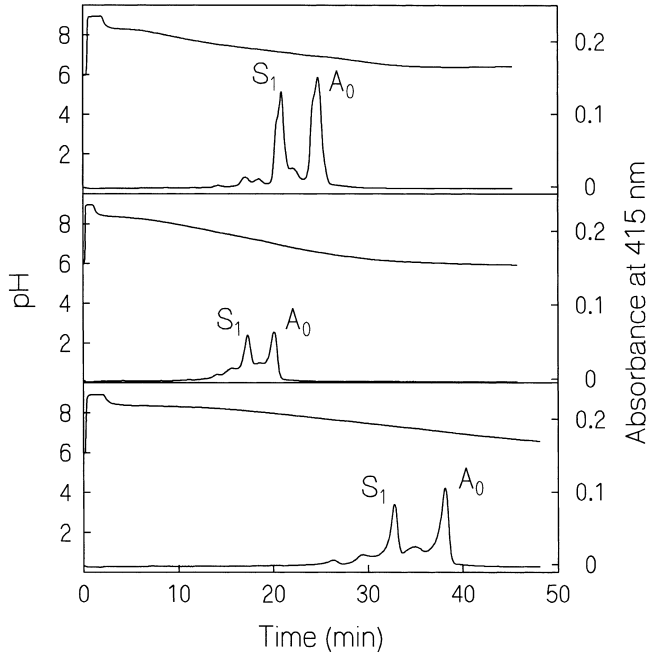

Figure 5. Chromatofocusing of 0.05 mg of a mixture of human hemoglobins A_0 and S_1. The presaturation buffer contained 10 mM diethanolamine at pH 9 titrated with HCl. The column was eluted with 2% (w/v) Polybuffer 96 at pH 6. Top: Mono Q column at a flow rate of 0.5 mL/min. Middle: Mono P column at a flow rate of 1 mL/min. Bottom: Mono P column at a flow rate of 0.5 mL/min.

Figure 6 illustrates the use of the PolySULFOETHYL A strong-acid cation-exchange column to produce an ascending pH gradient in the acidic range and separate proteins. As shown in the figure, a nearly linear pH gradient was produced between pH 3.7 and 7 after an initial small pH increase similar to the decrease shown in Figure 5. In addition, the three proteins ovalbumin, Lac A, and BSA were separated using the gradient shown. As illustrated, the three proteins are well separated, with a resolution that is generally better than that produced using a micropellicular weak-acid cation-exchange column as reported in Figure 1 of Kang and Frey (2003), which is again likely due to the higher Donnan potential obtained in the experiment shown.

Chromatofocusing of Peptides

General Considerations

Although reversed-phase chromatography (RPC) is extensively used for peptide separations (Mant and Hodges, 1991), this method exhibits a number of potential deficiencies, such as the inability to separate peptides with similar hydrophobicities or to preserve the activity of a biologically active peptide. There is consequently a need to develop alternative peptide separation methods that are complementary to RPC. For this purpose, cation-exchange or anion-exchange chromatography using a salt gradient have previously been investigated for separating basic and acidic peptides, respectively (Dizdaroglu, 1985; Isobe et al., 1982; Mant and Hodges, 1985; Takahashi et al., 1983). A more general IEC method has been reported by Alpert and Andrews (1988), who used cation-exchange chromatography with a mobile phase pH of 3.0. The method takes advantage of the fact that at pH 3 peptides lose their negative charges at aspartic and glutamic acid residues and the C-termini, and therefore become positively charged due to the presence of basic amino acid residues and the N-termini, so that nearly all peptides will adsorb onto a cation-exchange column packing.

Related work involving the separation of peptides using an unretained pH gradient formed by external mixing has been reported by Wall (1970), who employed a cation-exchange column packing and a linear pH gradient formed by mixing 0.1 M pyridine buffer at pH 3.5 as the starting buffer and 2 M pyridine at pH 5 as the final buffer, so that peptides were separated using a combined pH and ionic

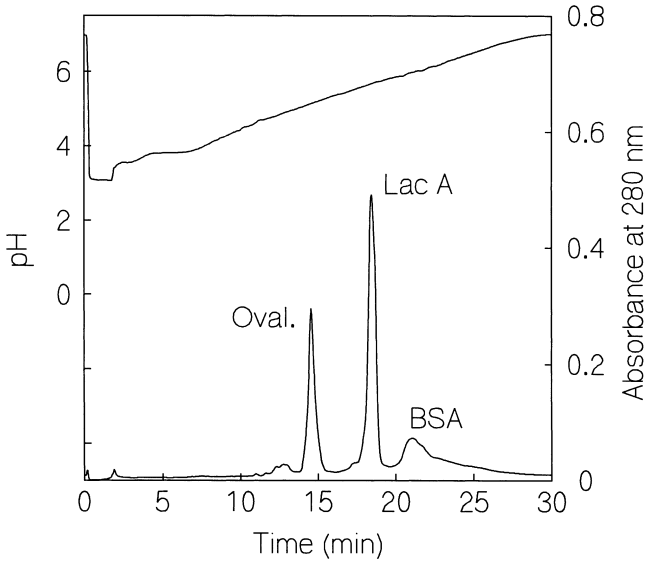

Figure 6. Chromatofocusing of 1.5 mg of a mixture of ovalbumin, β-lactoglobulin A, and bovine serum albumin using the PolySULFOETHYL A column. The column was presaturated with 10 mM NaH_2PO_4 at pH 3 and eluted with 10% (w/v) Polybuffer 74 at pH 7. The flow rate used was 1 mL/min.

strength gradient. Schroeder and Robertson (1965) also reported an ion-exchange method to separate tryptic peptides in which four eluents at different ionic strength and pH were introduced sequentially into an anion-exchange column, so that a pH gradient along with a stepwise salt gradient was produced. Although these two methods were moderately successful in separating peptides, neither of the methods exploits the characteristics of true chromatofocusing, where a pH gradient is formed dynamically inside the column so that focusing effects are maximized. The IEC method developed by Alpert and Andrews (1988) discussed above would similarly appear to offer opportunities for improvement in some situations since the separation achieved is based only on the difference in the charges at the basic residues. It is therefore reasonable to expect that chromatofocusing may have advantages in certain applications over previously investigated ion-exchange methods for separating peptides.

Selection of Column Packing

Although the separation of peptides arises in a wide variety of applications, in this study the analytical-scale separation of tryptic peptides will be considered due to its importance in protein sequencing. In order to select the optimal column packing for use in separating tryptic peptides by chromatofocusing, a number of additional considerations discussed by Alpert (1991) should be considered. In particular, when trypsin is used to digest a protein, the resulting peptides contain at least one basic amino acid residue, since trypsin cleaves the polypeptide chain at the carboxylic end of lysine and arginine residues (Croft, 1980). At pH 3, lysine, arginine, and histidine residues, as well as the N-termini, are positively charged, while aspartic acid and glutamic acid residues as well as C-termini are uncharged, resulting in a net charge of at least +2 for all tryptic peptides. Furthermore, if a strong-acid cation-exchange column is used at this pH, all of the peptides will bind to the column so that they can be individually eluted by increasing the mobile-phase pH to titrate the various acidic and basic residues. In this way, and in contrast to the case where the pH is fixed at 3 and an ionic-strength gradient is employed, all of the ionizable groups on the peptide participate in determining the elution behavior. Note in addition that a weak-acid cation-exchange column packing tends not to be suitable for use at pH 3 since the functional groups on the packing are largely uncharged at this pH.

Related considerations indicate that the use of an anion-exchange column packing, as opposed to a cation-exchange column packing, would require a pH of 13 for all the tryptic peptides to become negatively charged. However, at this pH even a strong-base anion-exchange packing would tend to become uncharged. The conclusion from all these considerations is that the use of a strong-acid cation-exchange column packing with an initial pH of 3, and with elution performed using a polyampholyte buffer, is the most promising route for separating tryptic peptides using chromatofocusing.

Comparison of Tryptic Peptide Separations Using Chromatofocusing and IEC With a Salt Gradient

Figure 7 shows the separation of a bovine hemoglobin tryptic digest using the PolySULFOETHYL A column to perform chromatofocusing and with a linear pH gradient produced as described above. In the experiment shown, the mobile phase contained 12.5% acetonitrile, as recommended by the column manufacturer to reduce hydrophobic interactions. As shown, eight peaks were detected in the gradual section of the gradient. In Figure 8 the same hemoglobin digest sample is separated using the same column as in Figure 7, but with the column operated at a fixed pH of 3 and with elution performed using a salt gradient. Note that in Figure 8 the eluted peptides were detected by their absorbance at both 214 and 280 nm, while in Figure 7 detection was performed only at 280 nm due to the fact that the polyampholyte buffer used produces a background absorbance at lower wavelengths.

As shown in Figure 8, the tryptic peptides of hemoglobin are well separated using IEC with a salt gradient. It can also be seen that only some of the peptides which are detected at 214 nm are also detected at 280 nm, due to the fact that only peptides having tryptophan or tyrosine residues are detectable at 280 nm, while all peptides are detectable at 214 nm. This indicates that although only eight peaks were observed in Figure 7, many more peptides are likely separated in the column effluent. If the peaks detected in Figure 7 and in Figure 8 at 280 nm are compared, it is evident that the separation of peptides using chromatofo-

cusing is comparable to that using IEC with a salt gradient, since in both cases the peak capacity, defined as the gradient time divided by the average peak width, is ~30, and in both cases approximately eight peaks are seen. In addition, since the separation achieved for the various peaks is different in the two figures, it is evident that chromatofocusing provides a complementary separation in comparison to IEC using a salt gradient.

The results in Figures 7 and 8 can also be compared to the number and sizes of peaks theoretically expected for the tryptic digest of bovine hemoglobin. Table I illustrates the expected tryptic peptides that absorb appreciably at 280 nm assuming complete digestion of the protein, along with the theoretically predicted p*I* values and molar absorbances at 280 nm. The p*I* values given in the table were determined as the pH where the net charge on a peptide is zero, assuming there are no interactions between ionizable groups. The ionization of each functional group on a peptide was determined using the Henderson-Hasselbalch equation (Stryer, 1975) with the pK_a values for the groups taken from Bjellqvist et al. (1993). The UV absorbance values shown in the table were determined as described by Gill and Hippel (1989). No attempt was made to correct the pK_a values for the presence of acetonitrile since, according to Espinosa et al. (2000), the amount of acetonitrile used should have a minor effect on the calculated p*I* values.

It can be seen that the peaks observed in Figures 7 and 8 are largely consistent with Table I, since in both figures three large peaks and at least four small peaks are observed, corresponding to the peptides with larger and smaller absorbances, respectively, in the table. However, incomplete tryptic digestion, multiple conformations of individual peptides, and co-elution of some of the expected peaks may be responsible for the minor differences between the results in Figures 7 and 8 and Table I. It can also be seen that the peptides in Figures 7 and 8 do not appear to elute in order of their isoelectric points, since the three peptides with the largest absorbances in Table I all have isoelectric points near 8.8, and therefore should have been the last peaks in the elution order if this order corresponds to the isoelectric points, whereas the three large peaks in Figures 7 and 8 are in the middle of the sequence of observed peaks.

As described earlier, one characteristic of using chromatofocusing for separating peptides is that detection at wavelengths less than 280 nm cannot be employed due to the background absorbance of the polyampholyte elution buffer at such wavelengths. However, all the peptides present could in principle be detected by using the

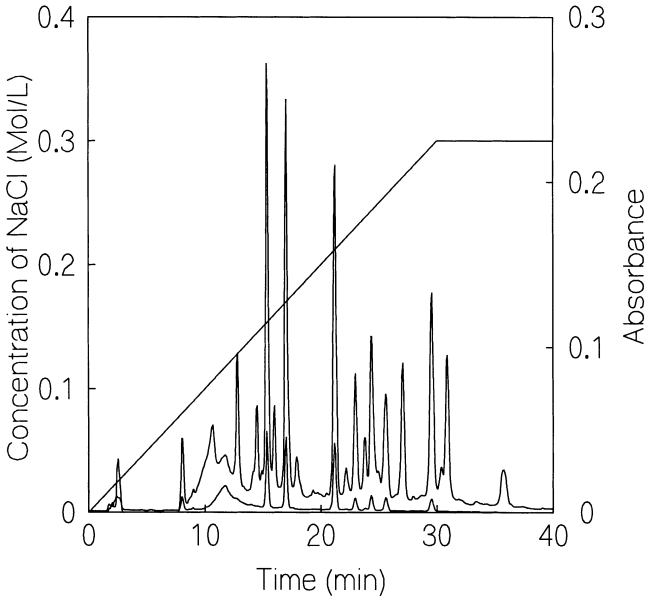

Figure 8. Ion-exchange chromatography of the tryptic digest of 0.05 mg bovine hemoglobin. Buffer A: 3.75 mM NaH_2PO_4 in 25% acetonitrile at pH 3. Buffer B: Buffer A with 0.3 M NaCl. The gradient used is also shown in the figure. A flow rate of 0.5 mL/min was used with the column effluent detected at the two wavelengths of 214 nm and 280 nm. Other conditions were the same as in Figure 6.

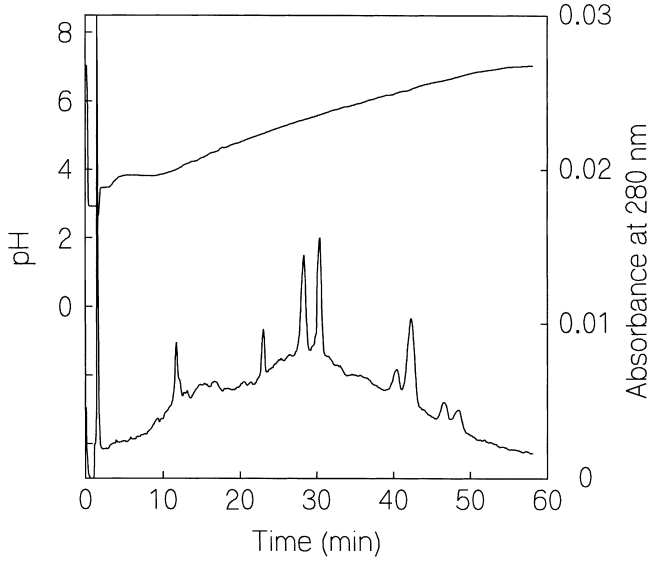

Figure 7. Chromatofocusing of the tryptic digest of 0.008 mg of bovine hemoglobin. The column was presaturated with 10 mM NaH_2PO_4 in 12.5% acetonitrile at pH 3 and eluted with 5% Polybuffer 74 in 12.5% acetonitrile at pH 7. Other conditions were the same as in Figure 6.

Table I. Tryptic peptides of bovine hemoglobin with an appreciable UV absorbance at 280 nm.

Peptide	p*I*	Absorbance at 280 nm (M^{-1} cm^{-1})
AAWGK	8.8	5690
VGGHAAEYGAEALER	4.5	1280
TYFPHFDLSHGSANVK	7.1	1280
YR	8.7	1280
LLVVYPWTNR	8.7	6970
YH	6.9	1280
AAVTAFWGK	8.8	5690

absorbance at 280 nm together with suitable pre- or postcolumn derivatization methods (Fermo et al., 1990; Gulati et al., 1999; Liu et al., 1999), or by employing mass-spectrometric instead of UV absorbance detection, so that the generality of the chromatofocusing method can be made comparable, if desired, to ion-exchange chromatography with a salt gradient.

Comparison of Tryptic Peptide Separations Using Chromatofocusing and Capillary Isoelectric Focusing

Figure 9 shows the chromatofocusing separation of a bovine cytochrome C tryptic digest. The expected tryptic peptides for bovine cytochrome C that have an appreciable absorbance at 280 nm assuming complete digestion are listed in Table II, along with the isoelectric points and absorbances calculated as described in the previous section. As illustrated, when using chromatofocusing five peaks are observed, four of which likely correspond to the four peptides listed in Table II. In addition, the two large peaks shown likely correspond to the incomplete tryptic cleavage or multiple conformations of the second peptide in Table II, since this peptide is the only one containing tryptophan. As was the case in Figures 7 and 8, the minor discrepancies between number and size of the peaks expected from Table II and those observed in Figure 9 is likely due not only to incomplete digestion of the protein and multiple conformations of peptides, but also to co-elution of some of the expected peptides.

The separation of the tryptic peptides of bovine cytochrome C was also performed by Mazzeo et al. (1993) using capillary isoelectric focusing (CIEF). Note that CIEF also has the same characteristic as the chromatofocusing method described above of having to use UV detection at wavelengths around 280 nm or greater due to the use of a polyampholyte buffer. Although Mazzeo et al. claimed to have observed seven tryptic peptides, many of which were apparently the result of nontryptic cleavages, several of the peaks they observed were extremely small, and the peak identification methods used were inconclusive. Nevertheless, since a comparable number of peaks are observed in Figure 9, it can be concluded that the separation achieved using the chromatofocusing technique described here is roughly comparable to that achieved using CIEF to separate the same tryptic digest.

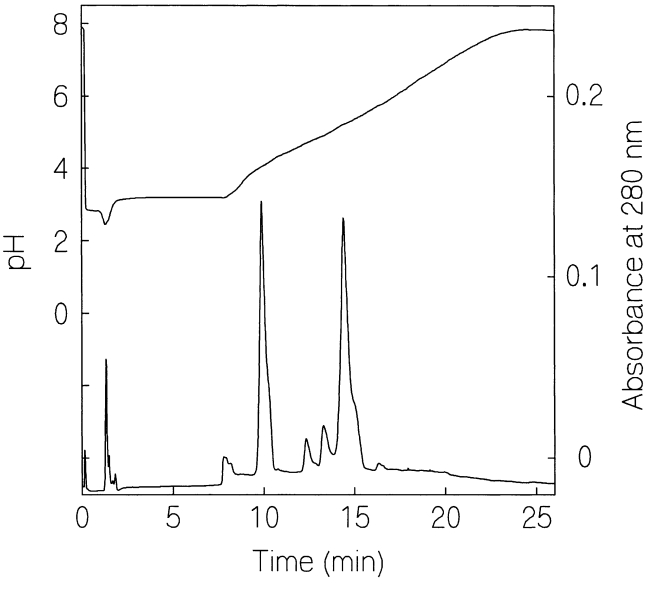

Figure 9. Chromatofocusing of the tryptic digest of 0.15 mg bovine cytochrome C. The column was presaturated with 10 mM citric acid in 25% acetonitrile at natural pH and eluted with 10% Polybuffer 74 in 25% acetonitrile at pH 8. Other conditions were the same as in Figure 6.

Table II. Tryptic peptides of bovine cytochrome C with an appreciable UV absorbance at 280 nm.

Peptide	p*I*	Absorbance at 280 nm (M^{-1} cm^{-1})
TGQAPGFSYTDANK	6.0	1280
GITWGEETLMEYLENPK	3.8	6970
YIPGTK	8.6	1280
EDLIAYLK	4.4	1280

The resolution achieved in Figures 7 and 9 where average baseline bandwidths are 0.1 and 0.2 pH units, respectively, are comparable to baseline bandwidths in terms of pH units observed by Mazzeo et al. (1993) in the study using CIEF described above, and to those observed by Mohan and Lee (2002), who investigated the use of CIEF for separating the tryptic digest of horse heart cytochrome C. Significantly smaller bandwidths were observed by Shen et al. (2000), who used specially coated capillaries to perform CIEF of a variety of peptides. However, regardless of which method yields a smaller bandwidth, the chromatofocusing method described here has several potential advantages over CIEF for peptide separations, including the fact that a second separation mechanism can be utilized to separate peptides with very similar electrostatic charge, and that peptides are less likely to precipitate in chromatofocusing than in CIEF, since in the former method peptides do not elute precisely at the true p*I*, where their solubility tends to be lowest.

Relation Between the pI and pI_{app} of Peptides

Table III and Figure 10 compare the measured pH for seven peptides of the column effluent when each peptide elutes during chromatofocusing, generally termed the apparent isoelectric point, with 25% acetonitrile in the mobile phase and with one of the peptides present in both the C-terminus free (i.e., acid) and C-terminus blocked (i.e., amide) form. The apparent isoelectric points for several of the peptides were also determined with 0% and 12.5% acetonitrile in the mobile phase. Also shown in the table are the values of the p*I* and d*z*/dpH calculated as described in the discussion related to Table I, with the latter parameter defined as five times the difference in the charge 0.1 pH units above and

below the measured value of pI_{app} with 25% acetonitrile in the eluent.

As shown in Table III and Figure 10, and in contrast to the results in Figure 7, all the peptides investigated elute in order of their calculated isoelectric points, and with pI_{app} values that are between 0.6 and 3.0 pH units less than their calculated pI values. Furthermore, since the amount of acetonitrile in the eluent has a relatively small effect on the pI_{app} values, hydrophobic interactions between the peptides and the column packing are likely unimportant for the relatively hydrophilic peptides considered here. The results also show that the C-terminus blocked form of the peptide YGGFL, which does not have an isoelectric point since the N-terminus is the only ionizable group present, has a pI_{app} value of 4.1, as compared to the unblocked form where the pI_{app} value is 3.4. This indicates that the titration of both the C-terminus and N-terminus of the unblocked form of the peptide combine to determine its elution behavior during chromatofocusing on the cation-exchange column packing used.

A more precise analysis of the relation between the pI and pI_{app} values for peptides can be obtained using the theoretical result of Sluyterman and Elgersma (1978), which can be written as:

$$pI - pI_{app} = \frac{\varphi}{4.6} - \frac{\ln(K_d)}{\varphi\,|dz/dpH|} \qquad (1)$$

where K_d is the distribution coefficient for the protein, defined as the mass of protein adsorbed per unit volume of the adsorbed phase divided by the concentration of the protein in the liquid phase, dz/dpH is the rate of change of the protein charge with pH, and φ is the logarithm of the ratio of hydrogen ion concentration in the fluid and adsorbed phases, which is equivalent to the dimensionless Donnan potential described by Sluyterman and Elgersma. Since φ is negative for the case of a cation exchanger, and if it is assumed that φ is constant for a given gradient, then a plot of pI − pI_{app} versus ln (K_d) / |dz/dpH| should be a straight line with a slope of $-1/\varphi$ and an intercept of φ/4.6. Since during chromatofocusing the peptide travels through the column at a fixed pH and liquid-phase composition, the distribution coefficient in Eq. (1) is given by:

$$K_d = (t - t_0)/(t_0\,P) \qquad (2)$$

where t is the retention time observed during chromatofocusing, t_0 is the retention time of an unretained eluite, taken to be the retention time of the peptide YGGFL at a mobile phase pH of 8, and P is the phase ratio, defined to be the ratio of the volumes of solid and liquid in the column.

Figure 11 illustrates the use of Eq. 1 to fit the experimental data in Table III. As shown, good agreement for all the peptides in Table III except the peptide GGYR is obtained with $\varphi = -2.2$, which is a reasonable value for this parameter since it corresponds to an ionic strength ratio between the stationary and mobile phase of exp(2.2) or 9.0. As also shown, the data for all seven peptides including the peptide GGYR can be fitted to the theoretically predicted line for $\varphi = -2.7$, but with significant scatter. This value for φ corresponds to an ionic strength ratio between the stationary and mobile phases of 14, and is somewhat higher than measured values of φ in related systems (Sluyterman and Wijdenes, 1978). This suggests that the behavior of the peptide GGYR is not entirely consistent with Eq. 1, although it is also possible that the inability of Eq. 1 to account for this peptide may be related to the small calculated value of |dz/dpH| for this case, which may result in a large relative error when determining the right side of the equation.

The results in Figures 10 and 11 can also be compared to results obtained by Mohan and Lee (2002) and by Shen et al. (2000), who employed CIEF for separating peptides.

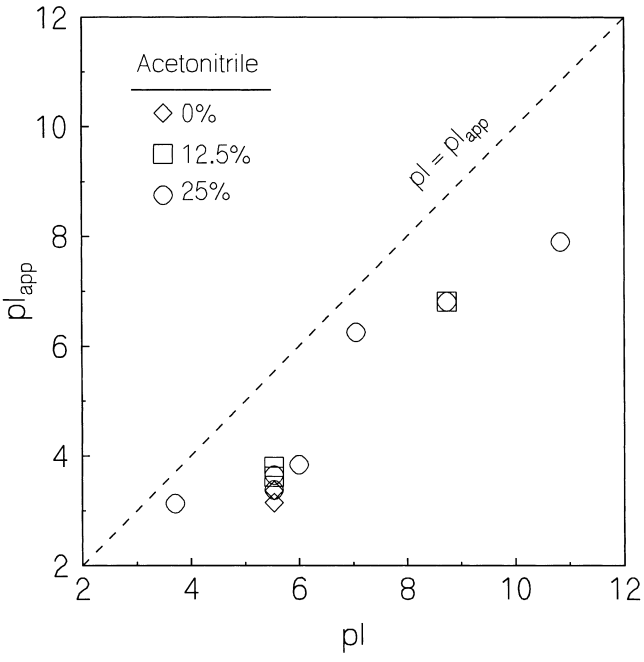

Figure 10. pI_{app} plotted versus pI for the peptides in Table III at several concentration levels of acetonitrile in the eluent. Experimental conditions were the same as in Figure 9.

Table III. Properties of selected peptides with an appreciable UV absorbance at 280 nm. The values of pI_{app} were determined with 25% acetonitrile in the eluent.

Peptide	pI_{app}	K_d	dz/dpH	pI	Absorbance at 280 nm (M^{-1} cm^{-1})
DRVYIHPFHL	6.2	35.7	−1.3	7.1	1280
CDPGYIGSR	3.8	20.4	−0.86	6.0	1280
YRPPGFSPFR	7.8	52.7	−0.53	10.8	1280
GGYR	6.8	38.0	−0.32	8.7	1280
WAGGDASGE	3.1	15.4	−0.70	3.7	5690
WG	3.6	16.2	−0.57	5.5	5690
YGGFL	3.4	15.6	−0.54	5.5	1280
YGGFL-NH2	4.1				1280

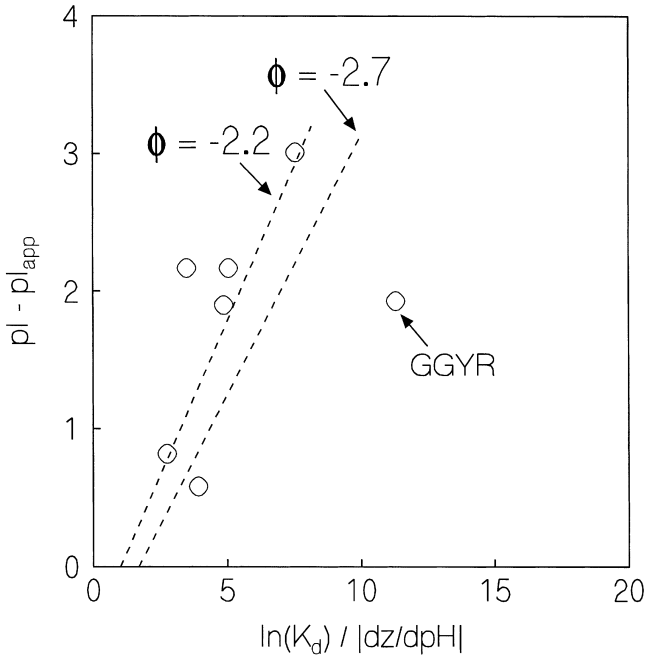

Figure 11. pI – pI_{app} plotted versus ln(K_d)/|dz/dpH| for the peptides in Table III. The dashed lines corresponds to Eq. 3 with $\varphi = -2.2$ and -2.7. The experimental conditions were the same as in Figure 9.

Although these workers observed that the migration times of tryptic peptides in CIEF were nearly always in order of their calculated isoelectric points, they also determined that the experimentally observed pI for certain peptides differed from the theoretical pI calculated by acid–base equilibrium by as much as 0.7 pH units. The results in Figure 11 therefore suggest that pI values calculated using acid–base equilibrium can in certain cases be used to identify peptides separated by chromatofocusing nearly as well as these values can be used to identify peptides in CIEF, provided that the relation between pI_{app} and pI is accounted for using an appropriate theory.

CONCLUSIONS

This study demonstrates that a linear or nearly linear pH gradient can be formed using a strong-acid or strong-base ion-exchange column packing if the column is presaturated with an unadsorbed buffering species, and then eluted with a polyampholyte elution buffer. The method takes advantage of the presence of small quantities of weak-electrolyte functional groups that generally exists on such column packings. The method was applied to the separation of human hemoglobin variants, bovine serum albumin, β-lactoglobulin A, and ovalbumin. The resolution obtained was found to be at least as good as, and in some cases better than, that achieved using chromatofocusing on weak-electrolyte ion-exchange column packing, probably due to the higher Donnan potential associated with strong-acid or strong-base column packings.

By taking advantage of the chromatofocusing technique just described and the characteristics of strong-acid cation-exchange column packings, tryptic peptides were separated for the first time using the technique of chromatofocusing. The peptide separation achieved was compared with that achieved using traditional ion-exchange chromatography using a salt gradient and capillary isoelectric focusing, and was found to provide a complementary separation to these alternative methods. It was also determined that for a test case of seven peptides the difference between the apparent isoelectric points measured by chromatofocusing and the calculated isoelectric points based on acid–base equilibrium agree at least qualitatively with theoretical relations developed by previous workers.

In a recent review of CIEF, Mantabe (1999) predicted that peptides of low to moderate size are unlikely to focus into narrow bands during isoelectric focusing due to the fact that the charge for such peptides approaches zero over a broad pH range. In contrast to this prediction, recent experimental studies (Mohan and Lee, 2002; Shen et al., 2000) have shown that small peptides focus into bands during CIEF that are as narrow as those for proteins. The present study has shown that a similar trends applies to the technique of chromatofocusing. In particular, peptides having as few as two residues, peptides having only the N- and C-termini as charged groups, and peptides having only an N-terminus charged group and with the C-terminus blocked, all were focused into relatively narrow bands by using a strong-acid cation-exchange column packing and a polyampholyte elution buffer to perform chromatofocusing.

NOMENCLATURE

A_i	acidic buffering species
B_i	basic buffering species
C_A	concentration in liquid phase, mol/L
I	inert ion
$K_{A,ads}$	adsorption equilibrium constant for buffering species
K_w	dissociation constant for water
N_A, N_B, N_R	number of weak-acid buffering species, weak-base buffering species, and column packing functional groups
P	phase ratio
q_A	concentration in particle, mol/L
t	time or elution time, s
t_0	elution time for an unadsorbed eluite, s
v	interstitial fluid velocity, cm/s
x	axial distance along column, cm
z	ionic charge

Greek Symbols

α	interstitial porosity
φ	dimensionless Donnan potential

Superscripts

–	negative charge
+	positive charge
0	uncharged

Subscripts

app	apparent value
A_i	acidic buffering species
B_i	basic buffering species

APPENDIX

This appendix describes briefly the procedure used in the numerical calculations shown in Figures 1–3. Additional details are given by Frey et al. (1995).

The acid–base reactions for weak-acid or weak-base buffering species having only monovalent ionic forms can be written:

$$A_i^o \rightleftharpoons A_i^- + H^+ \tag{A1}$$

$$B_i^+ \rightleftharpoons B_i^o + H^+ \tag{A2}$$

where A_i^- and A_i^o are the negatively charged and neutral forms of the acidic buffering species A_i, and B_i^+ and B_i^o are the positively and neutral charged forms of the basic buffering species B_i. The corresponding equilibrium relations can be written:

$$K_{A_i} = C_{A_i^-}\, C_{H^+}/C_{A_i^0} \tag{A3}$$

$$K_{B_i} = C_{B_i^o}\, C_{H^+}/C_{B_i^+} \tag{A4}$$

Equations A3 and A4 lead to the following expressions for the concentration of each individual ion present in terms of the total concentration of each buffering species considering all its forms, with the latter denoted by C_{A_i} and C_{B_i}:

$$C_{A_i^o} = \frac{C_{H^+}\, C_{A_i}}{C_{H^+} + K_{A_i}} \tag{A5}$$

$$C_{A_i^-} = \frac{K_{A_i}\, C_{A_i}}{C_{H^+} + K_{A_i}} \tag{A6}$$

$$C_{B^o} = \frac{K_{B_i}\, C_{B_i}}{C_{H^+} + K_{B_i}} \tag{A7}$$

$$C_{B_i^+} = \frac{C_{H^+}\, C_{B_i}}{C_{H^+} + K_{B_i}} \tag{A8}$$

The liquid-phase electroneutrality condition can be written using Eqs. A5–A8 as:

$$C_{I^+} - C_{I^-} - \sum_{i=1}^{N_A} \frac{K_{A_i}\, C_{A_i}}{K_{A_i} + C_{H^+}} + \sum_{i=1}^{N_B} \frac{C_{H^+}\, C_{B_i}}{K_{B_i} + C_{H^+}} + C_{H^+} - \frac{K_w}{C_{H^+}} = 0 \tag{A9}$$

where I^+ and I^- denote inert ions which do not participate in acid–base equilibrium, such as Na^+ or Cl^-.

At equilibrium the chemical potential of any electrically neutral combination of ions is the same in the adsorbed and liquid phases, in which case adsorption equilibrium for the species A_i^- can be written:

$$(q_{H^+})^{-z_{A_i^-}}\, q_{A_i^-} = K_{A_i^-,ads}\, (C_{H^+})^{-z_{A_i^-}}\, C_{A_i^-} \tag{A10}$$

with a similar expression applying to the species B_i^+. In Eq. A10, $q_{A_i^-}$ denotes the quantity of A_i^- in the adsorbed phase per unit volume of particle, and $K_{A_i^-,ads}$ is an adsorption equilibrium constant. For the case of a weak-base anion-exchange column packing, the ionizable functional groups attached to the adsorbent, represented by the concentration q_{R_i}, are included in the adsorbent electroneutrality condition, which can be written as:

$$q_{I^+} - q_{I^-} - \sum_{i=1}^{N_A} \frac{K_{A_i}\, q_{A_i}}{K_{A_i} + q_{H^+}} + \sum_{i=1}^{N_B} \frac{q_{H^-}\, q_{B_i}}{K_{B_i} + q_{H^+}} + \sum_{i=1}^{N_R} \frac{q_{H^+}\, q_{R_i}}{K_{R_i} + q_{H^+}} + q_{H^+} - \frac{K_{w,ads}}{q_{H^+}} = 0 \tag{A11}$$

For the particular case of a strong-base anion-exchange column packing, and if the concentrations of H^+, OH^-, and the adsorbed cations are assumed to be small compared to the adsorbed anions present, then the electroneutrality condition for the adsorbed phase can be written:

$$q_R = \sum_{i=1}^{N_A} q_{A_i^-} \tag{A12}$$

where q_R is the total ion-exchange capacity. Under these conditions Eqs. A6, A10, and A12 can be combined to yield:

$$q_{A_i^-} = \frac{q_R\, (C_{H^+} + K_{A_i})\, C_{A_i} \,/\, K_{A_i}}{\sum_{j=1}^{N_A} K_{A_i^-,ads}/K_{A_j^-,ads}\, (C_{H^+} + K_{A_j})\, C_{A_j} \,/\, K_{A_j}} \tag{A13}$$

Equation A13 is the usual relation for multicomponent anion-exchange equilibrium for weak acids which adsorb onto a strong-base ion-exchange column packing with the ratio $K_{A_i^-,ads}/K_{A_j^-,ads}$ being the ion-exchange selectivity between the ions A_i^- and A_j^-.

For the neutral forms of the buffering species where $z_{A_i^o} = 0$, Eq. A10 yields a linear adsorption relation, in which case the total amount of an adsorbed buffering species is given by adding the product $C_{A_i^o}\, K_{A_i^o,ads}$ to $q_{A_i^o}$, where $q_{A_i^-}$ is calculated as described above, and $K_{A_i^o,ads}$ is the adsorption equilibrium constant for the neutral form.

Since the total amount of the buffering species A_i satisfies a mass balance that does not include a term accounting for consumption by an acid–base reaction, and if the presence of the buffering species in the particle pores is ignored, the differential material-balance relation in the column for any buffering species can be written in terms of C_{A_i} and q_{A_i} as:

$$\alpha \frac{\partial C_{A_i}}{\partial t} + \alpha v \frac{\partial C_{A_i}}{\partial x} + (1 - \alpha) \frac{\partial q_{A_i}}{\partial t} = 0 \qquad \text{(A14)}$$

A similar equation also applies to all the inert ions which do not participate in acid–base equilibrium. For specified boundary and initial conditions, the numerical method of characteristics can be used to solve Eq. A14 simultaneously with Eqs. A5–A11 and the equations that describe the rate of interphase mass transfer.

We thank Andrew Alpert of PolyLC for helpful advice, and Jessica Soto Perez and Brooke Coley of UMBC for obtaining some of the data in Figures 10 and 11.

References

Alpert AJ. 1991. Ion-exchange high-performance liquid chromatography of peptides. In: Mant CT, Hodges RS, editors. HPLC of peptides and proteins: separation, analysis, and conformation, Boca Raton, FL: CRC Press. p 187–194.

Alpert AJ, Andrews PC. 1988. Cation-exchange chromatography of peptides on poly(2-sulfoethyl aspartamide)-silica. J Chromatogr 443: 85–96.

Amersham Pharmacia Biotech. 1981. Chromatofocusing with Polybuffer and PBE. Uppsala, Sweden: Amersham.

Bates RC, Kang X, Frey DD. 2000. High performance chromatofocusing using linear and concave pH gradients formed with simple buffer mixtures. I. Effect of buffer composition on the gradient shape. J Chromatogr A 890:25–36.

Bjellqvist B, Hughes GJ, Pasquali C, Paquet N, Ravier F, Sanchez JC, Frutiger S, Hochstrasser D. 1993. The focusing positions of polypeptides in immobilized pH gradients can be predicted from their amino acid sequences. Electrophoresis 14:1023–1031.

Croft LR. 1980. Handbook of protein sequence analysis: a compilation of amino acid sequences of proteins with an introduction to the methodology. New York: Wiley.

Dizdaroglu M. 1985. Weak anion-exchange high-performance liquid chromatography of peptides. J Chromatogr 334:49–69.

Espinosa S, Bosch E, Roses M. 2000. Retention of ionizable compounds in HPLC. 5. pH scales and the retention of acids and bases with acetronitrile-water mobile phases. Anal Chem 72:5193–5200.

Fermo I, De Vecchi E, Diomede L, Paroni R. 1990. Serum amino acid analysis with pre-column derivatization: comparison of the o-phthaldialdehyde and N,N-diethyl-2,4-dinitro-5-fluoroaniline methods. J Chromatogr 534:23–36.

Frey DD, Barnes A, Strong JC. 1995. Numerical studies of multicomponent chromatography using pH gradients. AIChE J 41:1171–1183.

Frey DD, Narahari CR, Butler CD. 2002. General local-equilibrium chromatographic theory for eluents containing adsorbing buffers. AIChE J 48:561–571.

Gill SC, von Hippel PH. 1989. Calculation of protein extinction coefficients from amino acid sequence data. Anal Biochem 182:319–326.

Gulati D, Bongers J, Burman S. 1999. RP-HPLC tryptic mapping of IgG1 proteins with post-column fluorescence derivatization. J Pharm Biomed Anal 21:887–893.

Isobe T, Takayasu T, Takai N, Okuyama T. 1982. High-performance liquid chromatography of peptides on a macroreticular cation-exchange resin: application to peptide mapping of Bence-Jones proteins. Anal Biochem 122:417–425.

Kang X. 2002. Novel methods of high-performance chromatofocusing. Ph.D. Dissertation, University of Maryland Baltimore County.

Kang X, Frey DD. 2002. Chromatofocusing using micropellicular column packings with computer-aided design of the elution buffer composition. Anal Chem 74:1038–1045.

Kang X, Frey DD. 2003. High-performance cation-exchange chromatofocusing of proteins. J Chromatogr A 991:117–128.

Liu H, Cho B, Strong R, Krull IS, Cohen S, Chan KC, Issaq HJ. 1999. Derivatization of peptides and small proteins for improved identification and detection in capillary zone electrophoresis. Anal Chim Acta 400:181–209.

Mant CT, Hodges RS. 1985. Separation of peptides by strong cation-exchange high-performance liquid chromatography. J Chromatogr 327:147–155.

Mant CT, Hodges RS. 1991. HPLC of peptides and proteins: separation, analysis and conformation. Boca Raton, FL: CRC Press.

Mantabe T. 1999. Capillary electrophoresis of proteins for proteomic studies. Electrophoresis 20:3116–3121.

Mazzeo JR, Martineau JA, Krull IS. 1993. Peptide mapping using EOF-Driven capillary isoelectric focusing. Anal Biochem 208:323–329.

Mohan D, Lee CS. 2002. Extension of separation range in capillary isoelectric focusing for resolving highly basic biomolecules. J Chromatogr A 979:271–276.

Schroeder WA, Robertson B. 1965. An improved gradient for ion exchange chromatography of peptides on Dowex-1. Anal Chem 37: 1583–1585.

Shen Y, Berger SJ, Anderson GA, Smith RD. 2000. High-efficiency capillary isoelectric focusing of peptides. Anal Chem 72:2154–2159.

Sluyterman LAÆ, Elgersma O. 1978. Chromatofocusing: isoelectric focusing on ion-exchange columns. I. General principles. J Chromatogr 150:17–30.

Sluyterman LAÆ, Wijdenes J. 1978. Chromatofocusing: isoelectric focusing on ion-exchange columns. II. Experimental verification. J Chromatogr 150:31–44.

Stryer L. 1975. Biochemistry. San Francisco: W.H. Freeman.

Takahashi N, Takahashi Y, Putnam FW. 1983. Two-dimensional high-performance liquid chromatography and chemical modification in the strategy of sequence analysis: complete amino acid sequence of the lambda light chain of human immunoglobulin. J Chromatogr 266: 511–522.

Wall RA. 1970. Separation of peptides on macroreticular ion exchangers. Anal Biochem 35:203–208.